

A Comparison of Fin Geometries for Heatsinks in Laminar Forced Convection: Part I - Round, Elliptical, and Plate Fins in Staggered and In-Line Configurations

Denpong Soodphakdee, Masud Behnia, and David Watabe Copeland*
School of Mechanical and Manufacturing Engineering
The University of New South Wales
Sydney 2052
Australia
Phone: 61-2-9385-4253
Fax: 61-2-9663-1222
e-mail: m.behnia@unsw.edu.au
*Showa Aluminum Corporation
480 Inuzuka, Oyama
Tochigi 323-8678
Japan

Abstract

In this study, the heat transfer performance of various commonly used fin geometries is compared. Realistic, manufacturable geometries are considered for minimizing thermal resistance at moderate laminar air velocities and pressure gradients. These consist of plate fins or pin fins, which can be round, elliptical, or square. The plate fins can be continuous (parallel plates) or staggered. The pin fins can be inline or staggered arrays.

In order to compare these various geometries, a set of standard conditions was required. The basis of comparison was chosen to be a circular array of 1mm diameter pin fins with a 2mm pitch. The pitch-to-width of the other geometries were chosen to provide equal ratios of fin cross-sectional area to base area. The pitch was fixed to provide the same wetted area per unit volume as that of the nominal case.

Analysis was simplified by three major assumptions. Heat transfer and fluid flow were assumed to be two-dimensional, with identical velocity and pressure distribution in the z-direction and similar temperature profiles. Flow and heat transfer were also assumed to be periodically developed, thereby permitting all but the first few rows of fins to be simulated by a model with similar velocity and temperature profiles at inlet and outlet. The ratio of solid to fluid thermal conductivity for aluminum and air is quite high, around 7000, permitting the fins to be modeled as isothermal surfaces rather than conjugate solids.

Each of these three assumptions reduced model complexity by about an order of magnitude. The CFD simulations were carried out on a two-dimensional computational domain bounded by planes of symmetry parallel to the flow. The air approach velocity was in the range of 0.5 to 5m/s. A comparison of heat transfer performance and pressure drop is presented. In general, the staggered plate fin geometry showed the highest heat transfer for a given combination of pressure gradient and flow rate. This method can be used to compare any repeating fin geometry in a ducted forced convection environment.

Key words:

Fin, Heatsink, Electronic Cooling, CFD, and Laminar Flow.

A Comparison of Fin Geometries for Heatsinks in Laminar Forced Convection: Part I - Round, Elliptical, and Plate Fins in Staggered and In-Line Configurations

Nomenclature

C_f	Friction coefficient
D_h	Hydraulic diameter (mm)
h	Surface heat transfer coefficient ($W/m^2 K$)
k	Thermal conductivity of air ($W/m K$)
Nu	Nusselt number
P_L	Lengthwise pitch (mm)
P_S	Spanwise pitch (mm)
Pr	Prandtl number
$(\Delta P/L)$	Pressure drop per unit length (Pa/m)
Re	Reynolds number
$v_{approach}$	Heatsink approach velocity (m/s)
w	Fin width (mm)

Greek symbol

λ_{flow}	Area of air flow passage per base area
$\lambda_{section}$	Fin cross-sectional area per base area
ρ	Density of air (kg/m^3)
μ	Dynamic viscosity of air ($kg/m s$)
ζ_s	Surface shear stress (Pa)
Π	Fin perimeter per base area (mm^{-1})

1. Introduction

With the increase of circuit density and power dissipation of integrated circuit chips and other microelectronic devices, electronic packagers have underlined the need for employing effective cooling devices and cooling methods to maintain the operating temperatures of electronics components at a safe and satisfactory level. The heatsink industry, traditionally the supplier of cooling products, is always searching for new technologies which enhance thermal performance with no cost penalties. For this reason, a comparison of various geometries of pin fin heatsinks is of interest and needs to be carried out to determine applicability as a general cooling product.

Operating conditions for microprocessor heatsinks have become considerably simpler than in the past. As the open boxes and undirected air flow representative of the low density packaging of early personal computers have disappeared, modern servers and workstations now feature fully ducted heatsinks with dedicated air moving devices. The dimensions of these heatsinks have also changed considerably, moving to narrower fin gaps approaching 1.5mm, tall fin heights approaching 50mm, and long flow lengths approaching 90mm.

The thermal network of a finned heatsink consists of conductive, radiative, and convective resistances. From the junction of the device, heat is transported by conduction from the device through the interface and into the heatsink from which heat is usually removed by means of convection and radiation. A literature survey shows very few studies on the thermal performance

of a pin fin heatsink. Chapman et al.¹ made a detailed comparison of thermal performance of different fin geometries. Crosscut pin fin and straight or parallel plate fins were investigated and compared with elliptical pin fin heatsink in their work. Fin efficiency and convective efficiency of different common fin geometries, shown in Figure 1, can be compared to help in selection of a heatsink.

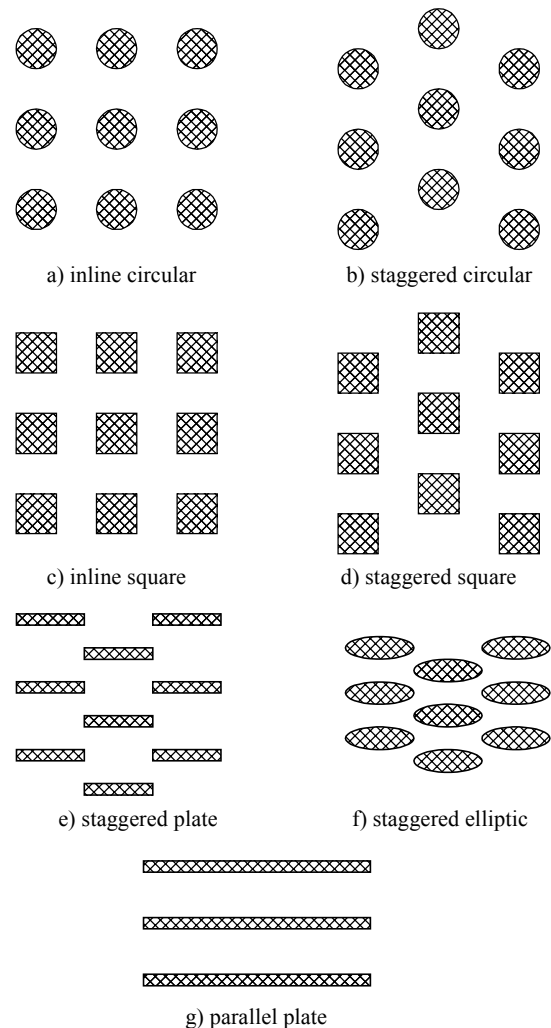


Figure 1. Schematic diagram of heatsinks.

For a comparison of heatsink geometries, equal wetted perimeter of the fins per base area will be used. The present work is meant to be a generalized comparison in which the effects of flow parameters (e.g. pressure drop) on the heatsink performance are investigated in terms of thermal resistance between the heatsink surfaces to the ambient air. The mechanisms that influence the heat transfer and pressure drop of various pin fin heatsinks need to be understood. The available literature on vari-

ous thermal performance studies is briefly reviewed in both parallel flow and impinging flow configurations. The numerical simulation procedure used in this work is described and results of various configurations are compared.

2. Literature Review

Comparisons of round-elliptical-square-parallel fins appear seldom in the literature. Wirtz et al.² were amongst the earliest ones to measure the performance of a pin fin heatsink. In their work, experimental results were reported on the thermal performance of model fan-sink assemblies consisting of a small axial flow fan for impingement of air on a square array of pin fins. Cylinder, square, and diamond shape cross-section pin-fins were considered. The overall heatsink thermal resistances, R , were evaluated at fixed applied pressure rise and fixed fan power. They concluded that cylindrical pin fins give the best overall fan-sink performance. Elliptical pin fin arrays were not studied in their investigation. In addition, only impinging flow drawn through the fin arrays was considered.

Sparrow and Larson³ performed experiments to determine per-fin heat transfer coefficients for a pin fin array situated in an oncoming longitudinal flow that turns to a cross-flow. They varied the geometric parameters of round fins including the fin height to diameter ratio (H/D) and the inter-fin pitch to diameter ratio (P/D). The pressure drop across the array was also measured and presented in dimensionless form relative to a specially defined velocity head, which gave a universal pressure drop result for all operating conditions. Subsequent to this study, they also compared the performance of different pin fin geometries⁴. However, the objective was to determine which fin height and inter-fin spacing yield the lowest overall thermal resistance for the array. The minimization of the resistance was sought under the constraint of constant pumping power for all candidate systems (i.e. those characterized by different H/D and P/D values) and for a uniform fin-to-airstream temperature difference for all fins in a given array.

In the experiments of Chapman et al.¹ with elliptical pin-fin heatsinks, results were obtained with aluminum heatsink made of extruded fin, crosscut rectangular fins, and elliptical fins in laminar air flow. All three heatsinks have equal volume, and the total surface area was also calculated to be nearly identical. The heatsink and ambient temperature difference was used to calculate thermal resistance. They supposed that the elliptical pin fin heatsink was designed to minimize the pressure loss across the heatsink by reducing the vortex effects and to enhance the thermal performance by maintaining large exposed surface area available for heat transfer. The optimal geometry of an array of fins that minimizes the thermal resistance between the substrate and the flow forced through the fins was reported by Bejan and Morega⁵. Both round pin fin arrays and staggered plate fin arrays were optimized in two steps, first the optimal fin thickness was selected and then the optimal size of fluid channel was de-

termined. They also compared the minimum thermal resistance of staggered plate arrays and parallel plate fins. Furthermore, the dimensionless pressure gradient was plotted against Reynolds number. Wirtz and Colban⁶ simulated electronic packages to compare the cooling performance of in-line and staggered plate arrays for both sparse and dense packaging configurations. They found that staggered arrays exhibit higher element heat transfer coefficients and friction factors than inline arrays at a given flow rate. However, no significant difference in performance was observed between staggered and inline configurations when they were compared based on either equal coolant flow pressure drop or pumping power. They did not change the element or channel geometry and therefore the effect of these parameters on their results is not known. In-line and staggered plate arrays were also investigated, both numerically and experimentally, by Sathyamurthy et al.⁷. They obtained a good agreement between their numerical results and experiments. Their results illustrated that the thermal performance of the staggered fin configuration was better than the planar fin configuration over the power and flow ranges examined. This enhanced thermal performance, however, was realized at the expense of an additional pressure drop. Heat transfer enhancement mechanisms in in-line and staggered parallel plate fin heat exchangers were also studied by Zhang et al.⁸ who examined the geometrical effects.

There are also a few reports on the thermal performance and the flow bypass effects of parallel plate fin arrays. Barrett and Obinelo⁹ studied tip clearance and spanwise spacing across a range of approach flow rates and fin densities. Wirtz et al.¹⁰ also studied the effect of flow bypass on the performance of longitudinal fin heatsinks. Iwasaki et al.¹¹ studied the cooling performance of this typical heatsink by using numerical, experimental and nodal network techniques. Keyes¹² studied forced convection through parallel plate fins, while natural convection in the same geometry was studied by Culham et al.¹³.

3. Objectives of the Present Study

Most of the previous studies on pin fins or parallel plate fin heatsinks have considered an individual geometry. Although Chapman et al.¹ compared elliptical pin fin heatsink with cross-cut pin fins and parallel plates, they used an equal volume of fins as the fixed parameter. Further, they did not include circular and square pin fins in their study. They mainly focused on investigating the advantages of elliptical pin fin heatsinks. In this study, some of the issues not considered in the previous works will be addressed. The objective is to numerically investigate the thermal performance of circular, square, elliptical pin fin, and parallel plate fin heatsinks and compare the results on a meaningful and fair basis. Both in-line and staggered arrays of different geometry fins are considered. In total, seven different two-dimensional geometries i.e., in-line cylindrical, staggered cylindrical, in-line square, staggered square, parallel plate, staggered plate, and staggered elliptical are modeled (see Figure 1).

Numerical simulations are performed using FLUENT Version 5, a commercially available general-purpose Computational Fluid Dynamics (CFD) code¹⁴. The code uses the Finite Volume method approach and employs the SIMPLEC velocity-pressure coupling algorithm¹⁵. The approach velocity range considered only covers laminar flow conditions. An extension to turbulent flow will be considered in the future.

4. Parameters and Geometry

With the changing dimensions, simplification of boundary conditions has become possible. The absence of bypass permits use of a computational domain no larger than the heatsink. The high flow resistance permits use of a single half-channel to model the entire heatsink. The high channel aspect ratio (nearly 30:1) allows an approximation as parallel plates and therefore justifies a two-dimensional model. Most of the long channel, with length approaching 30 hydraulic diameters, may be assumed to be in the fully developed flow regime.

As noted above, seven different geometries have been considered. In order to make a comparison for the purpose of optimizing heat transfer rate, some parameters are fixed for all geometries. These are: (i) the fin cross-sectional area per base area, (ii) the wetted perimeter per base area, and (iii) the area for air flow passage per base area. The commonly used in-line circular array of fins with 1mm pin diameter (w) and a 2mm pitch ($P_S=P_L$) has been selected to be the base case for comparison (see Figure 2). This yields a fin cross-sectional area per base area as shown below. It should be noted that, in essence, for a given fin base area the three parameters: fin cross-sectional area, wetted perimeter and flow passage area are fixed. However, for the sake of generalizing a fair and meaningful approach, the parameters in this case are all based on a per unit base area.

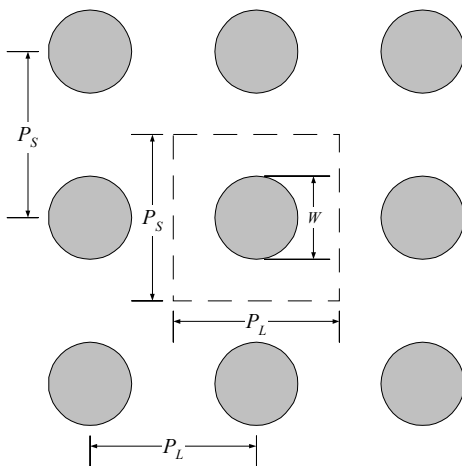


Figure 2. In-line circular pin fin.

$$\lambda_{section} = \frac{\pi w^2/4}{P_S P_L} = \frac{\pi(1)^2/4}{2 \times 2} = 0.19635 \quad (\approx 19.6\%)$$

This parameter is essentially representing the fin cross-sectional area. Similarly, the area for air flow passage (per base area) and the wetted perimeter per base area are as representing as follows,

$$\lambda_{flow} = 1 - \lambda_{section} = 1 - \frac{\pi w^2/4}{P_S P_L} = 0.80365$$

By fixing these three parameters in this work, the effect of varying other parameters on the performance of fins is demonstrated. The hydraulic diameter for internal flow is determined from the flow passage area as follows,

$$D_h = \frac{4 \times \lambda_{flow}}{\Pi} = \frac{4 \times 0.80365}{0.78540} = 4.0929 \text{ mm}$$

For the case of parallel plates, this is equal to twice the plate spacing. This differs from the traditional use of tube diameter for circular tube arrays, but is necessary to reflect the nature of internal flow and permit comparison of a variety of fin geometries. The Reynolds number (Re) is based on the hydraulic diameter and the heatsink approach velocity, $v_{approach}$ as shown in Figure 1. For the Nusselt number, the bulk inlet temperature is used as the reference for heat transfer coefficient calculations, shown in Figure 2.

$$Re = \frac{\rho v_{approach} D_h}{\mu} \tag{1}$$

$$Nu = \frac{h D_h}{k} \tag{2}$$

Friction coefficient, C_p is calculated as a function of pressure gradient in heatsink using heatsink approach velocity as reference. The friction coefficient for external flow over an array of fins is defined as in Figure 3.

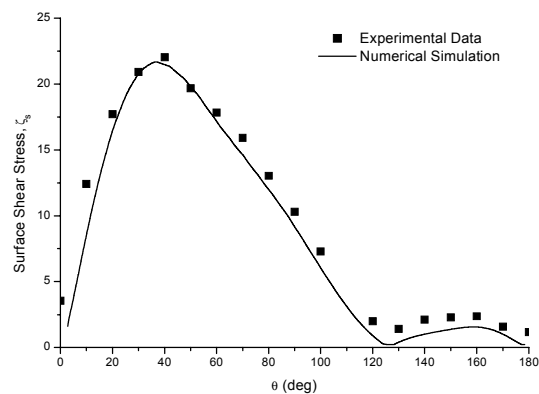


Figure 3. Comparison of experimental and numerical surface shear stress distributions at $Re=54$ for staggered array of tubes.

$$C_f = \frac{(\Delta P/L)D_h}{4\left(\frac{1}{2}\rho v_{\text{approach}}^2\right)} = \frac{(\Delta P/L)D_h}{2\rho v_{\text{approach}}^2} \quad (3)$$

where $(\Delta P/L)$ is the pressure gradient (pressure drop in the fin array per unit length).

5. CFD Modeling and Validation

The governing equations are those of two-dimensional continuity, Navier-Stokes and the energy equation in their incompressible laminar form. These equations are well known and will not be repeated in this publication. The details and solution method are given in Reference¹⁴. However, since the conventional fully developed flow condition cannot be applied in the case of flow in pin fin array. The periodically fully developed flow condition proposed by Patankar et al.¹⁶, implemented in FLUENT, was used. Some simplifying assumptions were made for the simulation. Firstly, as mentioned above, all but first few rows of fins are periodically fully developed flow, so a small unit cell measuring one spanwise pitch (P_s) and two lengthwise pitches (P_L), were used to model the entire heatsink. Secondly, the fins have minimal taper and wall thickness and free stream effects are confined to small regions at the end of the fins, permitting a two-dimensional model to be used. Finally, an aluminum heatsink placed in air has a solid/fluid thermal conductivity ratio of 7000, and temperature gradients in the fins are negligible in all directions except normal to the heatsink base. With both of these considerations, an isothermal model modified by an analytical fin efficiency is justified and used here. In the computational domain, in direction of the flow, a periodic boundary condition is adopted. While in the transverse direction, symmetry condition is used. For the thermal boundary condition on the solid surfaces, an isothermal condition is imposed. All fluid (i.e. air) properties are assumed to be constant.

The FLUENT Version 5 CFD code was used for the simulations. The simulation procedure was started with pre-processing. The computational mesh was generated using triangular elements. In order to accurately resolve the solution fields in the high gradient regions, the grid was stretched. In addition to stretching, adaptive solution algorithms were used to ensure an accurate resolution of the temperature and velocity gradients. The discretization scheme was second order accurate. A SIMPLEC velocity-pressure coupling multigrid solution procedure was used. For the simulations presented here, depending on the geometry used, fine meshes of up to 50000 elements were used. The flow field and heat transfer were determined by iteratively solving the governing momentum and energy equations. The under-relaxation factors were first set at low values to stabilize the calculation process, and were increased to speed up the convergence. The normalized residuals were set at 10^{-4} for velocity compo-

nents and at 10^{-7} for energy equation, which proved to be adequate.

For the purpose of the validation of the solution procedure, it is essential that CFD simulations be compared with experimental data. However, detailed local measurements for most of the heatsink fin geometries simulated in this work are not available in the literature. Therefore, the reasonably relevant geometries for which published experimental data are available were chosen. Two sets of data for inline and staggered tube banks, both extensively studied, were selected for validation^{17, 18}.

A comparison of the local dimensionless surface shear stress for the flow around the 7th tube row of a staggered tube bank with a longitudinal and transverse pitch of 2 is presented in Figure 3. It is noted that, considering the accuracy of the measurements, the agreement is very good. In particular, the first and second peak is very accurately resolved in the simulation.

The variation of the averaged dimensionless heat transfer coefficient with Reynolds number in an inline tube bank geometry is presented in Figure 4. The second row of tubes with a transverse and longitudinal pitch of 1.5 was simulated here. It is noted for the sake of comparison with experiments the Reynolds number is based on the tube diameter. The agreement is very good and the trend of simulated results correctly shows the change of slope observed in the experiments.

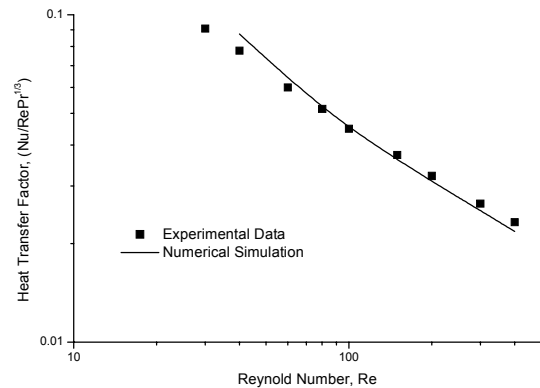


Figure 4. Comparison of experimental and numerical heat transfer factor for an in-line array of tubes.

The comparison of these simulations with experimental data validates the solution procedure. It can therefore be concluded that the CFD code can be used to solve the flow and temperature fields for similar geometries and conditions.

6. Results

For each geometry, results were obtained at various air velocities in the range of 0.5 to 5 m/s. Since the hydraulic diameter was fixed as noted previously, this covered a fixed range of

A Comparison of Fin Geometries for Heatsinks in Laminar Forced Convection: Part I - Round, Elliptical, and Plate Fins in Staggered and In-Line Configurations

Reynolds number for each geometry. A sample of the computational domain and grid for the circular fin geometry is shown in Figure 5. The horizontal boundaries of the computational domain are symmetry boundary conditions. The computational module is assumed to be well within the bank of fins and hence the inlet and outlet boundaries are considered to be of a periodic type. For clarity, only the grid in the vicinity of the fin is shown in this Figure.

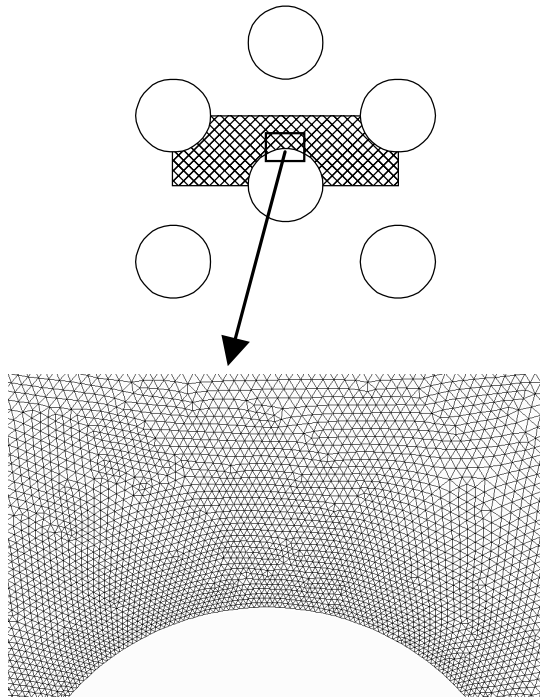


Figure 5. Computational domain and the grid near the circular fin surface.

In order to ensure mesh-independent solutions, the mesh was checked at the highest Reynolds number by refining it as well as using local solution adaptation features of the code. In performing the mesh refinement, once the Nusselt number changed by less than 0.5% the grid was considered to be fine enough. This resulted in a maximum number of 50,000 elements for the most sensitive case. A sample of computed contours of axial velocity and temperature distribution for the base case (i.e. in-line circular fin) at $Re = 260$ is shown in Figure 6.

A comparison of the average Nusselt number variation with Reynolds number for various geometries is shown in Figures 7 and 8. For clarity, the results are not plotted on a single graph and are grouped into two. The in-line and staggered geometries are compared in Figure 7, and the various staggered fin types are compared in Figure 8. For each geometry, seven simulations were carried out by varying the airflow rate. The curves represent the lines of best fit through the seven points obtained in the simulations. It can be noted that the staggered circular fin shape yields the highest Nusselt number at all Reynolds numbers in the

range considered here. The lowest Nusselt number is for that of parallel plate and staggered plate arrangements, with the former showing a milder Reynolds number dependence than the latter. Figure 7 clearly shows that the parallel plate configuration yields to a Nusselt number which is much lower than the other configurations. It is interesting to note that the staggered elliptic fins are only marginally better than the staggered plate.

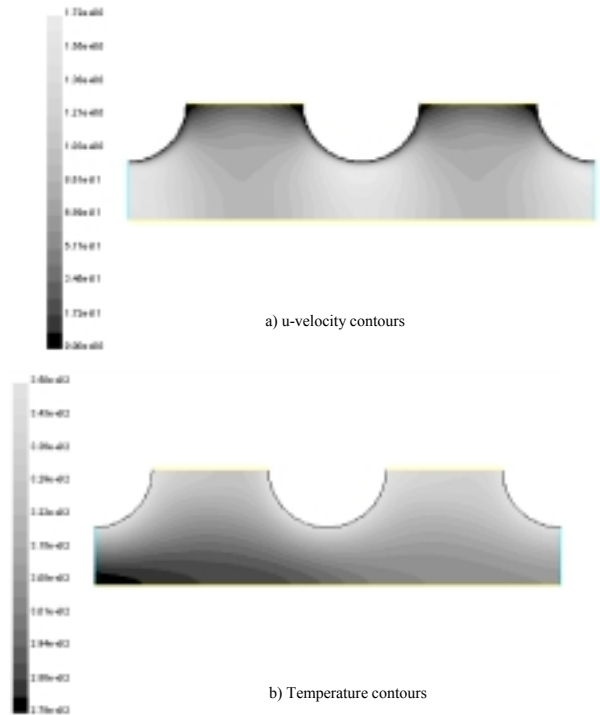


Figure 6. Contours of u-velocity and temperature at $Re=260$.

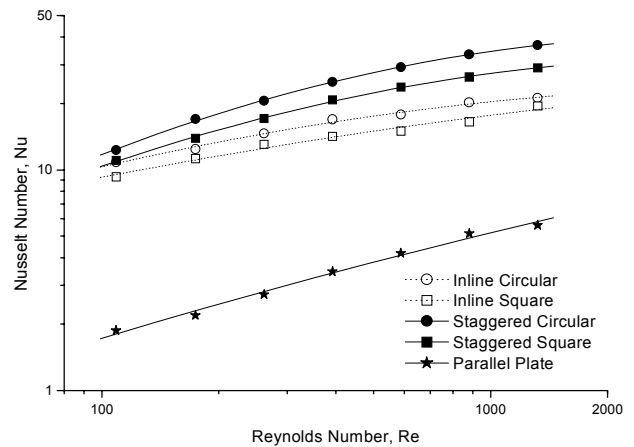


Figure 7. Nusselt number versus Reynolds number for various fin geometry.

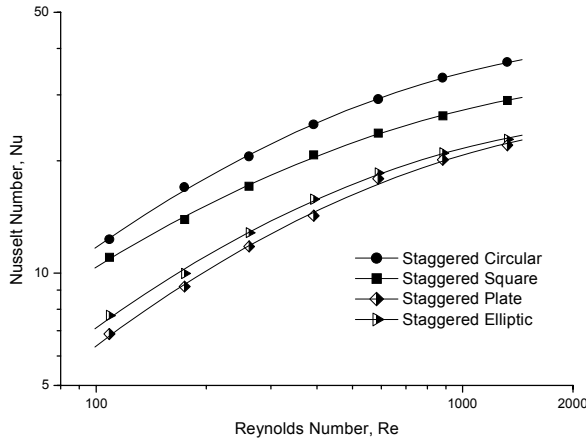


Figure 8. Nusselt number versus Reynolds number for staggered fins.

In order to compare the fan power requirements of each geometry, the friction coefficient was plotted in Figure 9. The relative differences are nearly constant for all geometries throughout the range of velocities studied except for the parallel plate. The parallel plate exhibits the lowest pressure drop, whereas the staggered circular is the worst configuration (note that this has the highest heat transfer coefficient).

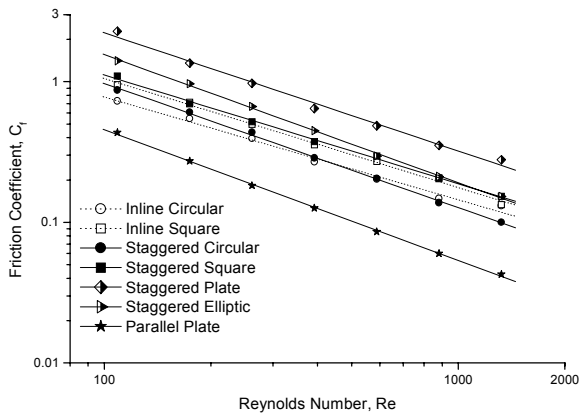


Figure 9. Friction coefficient versus Reynolds number for various fins.

The heat transfer coefficient versus pressure gradient is shown in Figure 10. It is noted that the results are presented in this figure in dimensional form. The seven points on each line of best fit correspond to the seven Reynolds numbers simulated (i.e. $Re=110, 175, 260, 390, 590, 880,$ and 1320). The different geometries can then be compared in terms of thermal performance as a function of pressure drop. At a given pressure drop, the staggered plate and staggered elliptic heatsinks permit more air-flow. At lower flow rates, these geometries provide better heat transfer performance. At higher values of pressure gradient, above 1 Pa/cm , the staggered circular and square geometries show the

highest performance. Throughout the range of flow rates studied, the in-line geometries performed poorly.

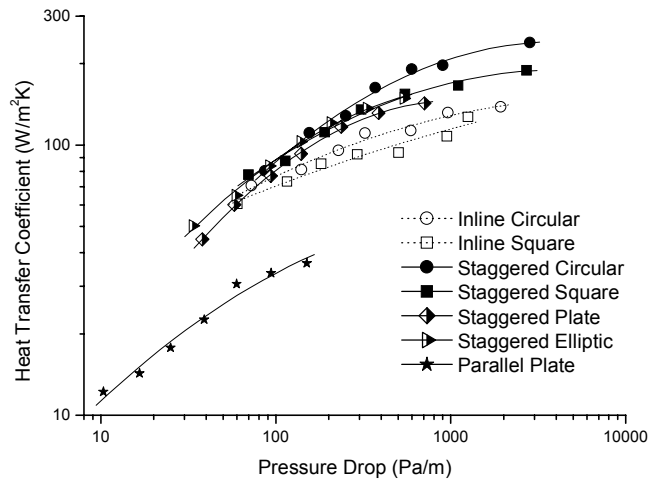


Figure 10. Variation of pressure drop versus heat transfer coefficient.

In all cases, circular pin fins outperform square pin fins and elliptical fins outperform plate fins. Throughout the range of velocities, staggered plate fins show higher pressure drop and lower heat transfer than staggered elliptic fins. Square pins have pressure drop comparable to that of circular pins but lower heat transfer.

Figure 11 shows heat transfer plotted against pumping power. This results in shifts in the relative performance of the various geometries. The staggered plate configuration offers the highest conductance at fixed pumping power throughout the range of flow rates studied, while parallel plate fins offers the lowest. In general, the geometries providing the highest heat transfer coefficients do so at the expense of excessive pressure drop.

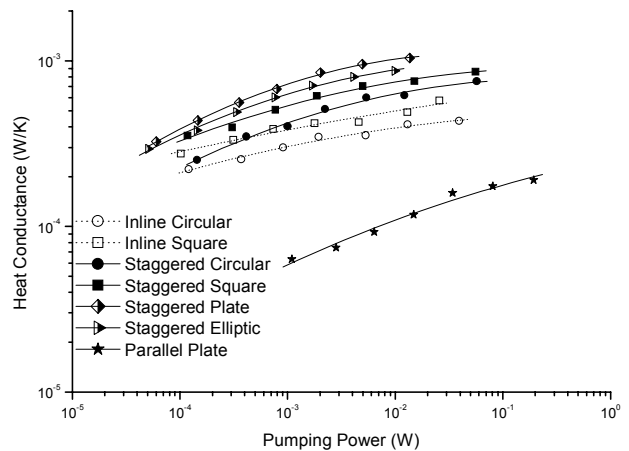


Figure 11. Variation of pumping power versus heat conductance.

7. Conclusions

A comparison of various heatsink geometries has been attempted. These were simplified by assuming periodically developed two-dimensional flow and isothermal heat transfer surfaces. In general, it is found that rounded geometries outperform similar sharp-edged fin shapes. In all cases, staggered geometries perform better than inline. At lower values of pressure drop and pumping power, elliptical fins work best. At higher values, round pin fins offer highest performance. The small number of previous studies of these fin geometries, usually comparing only two at a single operating point, have demonstrated some of the conclusions reached here. These conclusions are qualitatively known, but the current study quantifies these effects and compares various geometries with equal values of fin/base area ratio and lengthwise/spanwise pitch ratio. In this study, differences in thermal and hydraulic performance of all seven fin geometries over a wide range of Reynolds numbers were quantified.

A three-dimensional conjugate problem has been studied with a two-dimensional isothermal model. Copeland et al.¹⁹ compared conjugate and isothermal results for a silicon microchannel heatsink using fluorocarbon as the coolant, and found an isothermal approximation to be adequate. In their case, the conjugate model required more than 20 times as much computation time. In the current model, the ratio of thermal conductivities of solid and fluid (aluminum and air) is even higher, resulting in even slower convergence of the model, and making the isothermal approximation even more valid. The two-dimensional, periodically developed approximation also greatly simplifies a complicated situation. In a fully ducted environment which minimizes bypass, the flow field will be nearly constant in the z-direction, disturbed only at the base and end of the fins. The periodically developed boundary condition will underestimate pressure drop and heat transfer only in the first few rows of fins. Both of these simplifying assumptions permit a more general comparison of the various fin geometries.

In this study, the ratio of fin cross-sectional area to base area was kept constant at just below 20%. Additionally, the lengthwise fin pitch was held equal to the spanwise pitch. Both of these constraints can be relaxed in future studies, increasing the number of parameters available and greatly increasing the complexity of the problem. Another issue is that of the periodic boundary condition. This provides a conservative lower bound on both heat transfer and pressure drop. The degrees to which these are underpredicted depend on the fin geometries and the length of the heatsink relative to the entry region.

References

1. C. L. Chapman, S. Lee, and B. L. Schmidt, "Thermal Performance of an Elliptical Pin Fin Heatsink," *Proceedings of the Tenth IEEE Semiconductor Thermal Measurement and Management Symposium (Semi-Therm)*, San José, California, February 1-3, pp. 24-31, 1994.
2. R. A. Wirtz, R. Sohal, and H. Wang, "Thermal Performance of Pin-Fin Fan-Sink Assemblies," *Transactions of the ASME, Journal of Electronic Packaging*, Vol. 119, No. 1, pp. 26-31, March 1997.
3. E. M. Sparrow and E. D. Larson, "Heat Transfer from Pin-Fins Situated in an Oncoming Longitudinal Flow which Turns to Crossflow," *International Journal of Heat Mass Transfer*, Vol. 25, No. 5, pp. 603-614, 1982.
4. E. D. Larson and E. M. Sparrow, "Shorter Communications in Heat Transfer from Pin-Fins Situated in an Oncoming Longitudinal Flow which Turns to Crossflow," *International Journal of Heat and Mass Transfer*, Vol. 25, No. 5, pp. 723-725, 1982.
5. A. Bejan and A. M. Morega, "Optimal Arrays of Pin Fins and Plate Fins in Laminar Forced Convection," *Transactions of the ASME, Journal of Heat Transfer*, Vol. 115, pp. 75-81, February 1993.
6. R. A. Wirtz and D. M. Colban, "Comparison of the Cooling Performance of Staggered and In-Line Arrays of Electronic Packages," *Transactions of the ASME, Journal of Electronic Packaging*, Vol. 118, No. 1, pp. 27-30, March 1996.
7. P. Sathyamurthy, P.W. Runstadler, and S. Lee, "Numerical and Experimental Evaluation of Planar and Staggered Heat Sinks," *Proceedings of the Fifth InterSociety Conference on Thermal Phenomena in Electronic Packaging (Itherm)*, Orlando, Florida, May 28 - June 1, pp. 132-139, 1996.
8. L. W. Zhang et al., "Heat Transfer Enhancement Mechanisms in Inline and Staggered Parallel-Plate Fin Heat Exchanger," *International Journal of Heat and Mass Transfer*, Vol. 40, No. 10, pp. 2307-2325, 1997.
9. A. V. Barrett and I. F. Obinelo, "Characterization of Longitudinal Fin Heatsink Thermal Performance and Flow Bypass Effects Through CFD Methods," *Proceedings of the Thirteenth IEEE Semiconductor Thermal Measurement and Management Symposium (Semi-Therm)*, Austin, Texas, January 28-30, pp. 158-164, 1997.
10. R. A. Wirtz, W. Chen, and R. Zhou, "Effect of Flow Bypass on the Performance of Longitudinal Fin Heatsinks," *Transactions of the ASME, Journal of Electronic Packaging*, Vol. 116, pp. 206-211, September 1994.
11. H. Iwasaki, T. Sasaki, and M. Ishizuka, "Cooling Performance of Plate Fins for Multichip Modules," *IEEE Transaction on Components, Packaging, and Manufacturing Technology - Part A*, Vol. 18, No. 3, pp. 592-595, September 1995.

12. R.W. Keyes, "Heat Transfer in Forced Convection Through Fins," *IEEE Transactions on Electron Devices*, Vol. 31, No. 9, pp. 1218-1221, September 1984.
13. J. R. Culham, M. M. Yovanovich, and S. Lee, "Thermal Modeling of Isothermal Cuboids and Rectangular Heatsinks Cooled by Natural Convection," *IEEE Transactions on Components, Packaging, and Manufacturing Technology -Part A*, Vol. 18, No. 3, pp. 559-566, September 1995.
14. FLUENT/UNS User's Guide, Fluent Incorporated, Lebanon, New Hampshire, 1999.
15. J. P. Van Doormall and G. D. Raithby, "Enhancements of the SIMPLE Method for Predicting Incompressible Fluid Flows", *Numerical Heat Transfer*, Vol. 7, pp. 147-163, 1984.
16. S. V. Patankar, C. H. Liu, and E. M. Sparrow, "Fully Developed Flow and Heat Transfer in Ducts Having Streamwise-Periodic Variations of Cross-Sectional Area", *Transactions of the ASME, Journal of Heat Transfer*, Vol. 99, pp.180-186, May 1977.
17. O. P. Bergelin, G. A. Brown, and S. C. Doberstein, "Heat Transfer and Fluid Friction during Flow across Banks of Tubes -IV", *Transactions of the ASME*, Vol. 74, pp. 953-960, August 1952.
18. T. Nishimura, H. Itoh, K. Ohya, and H. Miyashita, "Experimental Validation of Numerical Analysis of Flow across Tube Banks for Laminar Flow", *Journal of Chemical Engineering of Japan*, Vol. 24, No. 5, pp. 666-669, 1991.
19. D. Copeland, M. Behnia and W. Nakayama, "Manifold Microchannel Heatsinks: Conjugate and Extended Models", *Proceedings of the Fifth InterSociety Conference on Thermal Phenomena in Electronic Systems, (Itherm)*, Orlando, Florida, May 28 – June 1, pp. 251-257, 1996.